Enhanced Cavity Optomechanics with Quantum-Well Exciton Polaritons

N. Carlon Zambon,[1,*,†,‖] Z. Denis,[2,*,‡] R. De Oliveira,[2] S. Ravets,[1] C. Ciuti,[2] I. Favero,[2] and J. Bloch[1]
[1]Centre de Nanosciences et de Nanotechnologies (C2N), CNRS-Université Paris-Saclay, 91120 Palaiseau, France
[2]Université Paris Cité, CNRS, Matériaux et Phénomènes Quantiques, F-75013 Paris, France

(Received 24 February 2022; accepted 18 July 2022; published 25 August 2022)

Semiconductor microresonators embedding quantum wells can host tightly confined and mutually interacting excitonic, optical, and mechanical modes at once. We theoretically investigate the case where the system operates in the strong exciton-photon coupling regime, while the optical and excitonic resonances are parametrically modulated by the interaction with a mechanical mode. Owing to the large exciton-phonon coupling at play in semiconductors, we predict an enhancement of polariton-phonon interactions by 2 orders of magnitude with respect to mere optomechanical coupling: a near-unity single-polariton quantum cooperativity is within reach for current semiconductor resonator platforms. We further analyze how polariton nonlinearities affect dynamical backaction, modifying the capability to cool or amplify the mechanical motion.

DOI: 10.1103/PhysRevLett.129.093603

Optomechanical interactions represent an essential resource for augmented sensing techniques [1–3], in nonlinear optics [4–7], and to investigate quantum phenomena in macroscopic systems [8–11]. Furthermore, coherent phonon scattering is an appealing route to implement microwave-to-optical transducers [12–14], necessary to interface distant superconducting quantum hardware [15–18]. To these ends, a key figure of merit is the single-photon quantum cooperativity $C_q = C_0/n_{\mathrm{th}}$, where C_0 is the single-photon cooperativity and n_{th} is the mechanical mode thermal occupation. It gauges the ability to coherently control the mechanical state with a single intracavity photon before environment-induced dephasing sets in [19]. Maximizing $C_0 = 4g_0^2/\kappa\Gamma$ requires small optical (κ) and mechanical (Γ) dissipation rates and large single-photon optomechanical couplings (g_0), while n_{th} can be reduced using high-frequency mechanical resonators [20–22] and operating them at cryogenic temperatures [23,24]. Recent works achieved a large cooperativity by engineering resonators with ultralow mechanical and optical losses [22,25]. A complementary approach is to devise solutions to enhance optomechanical interactions while working with modest optical and mechanical quality factors. Less stringent bandwidth limitations in optomechanical conversion are thereby imposed [26], while suppressing optical heating and added noise [22].

In direct-band-gap semiconductors, photoelastic effects typically dominate optomechanical coupling [27] and are greatly enhanced near electronic resonances of the material [28]. Moreover, in micromechanical resonators hosting quantum wells (QWs), electronic transitions can be tailored to boost carrier-mediated mechanical effects [29]. In both cases, an increase of optical absorption affects the cavity finesse and favors photothermal effects, while mechanical dephasing can be activated through photogenerated carriers [30,31]. In this context, GaAs-based resonators engineered to simultaneously confine photons, phonons, and QW excitons offer an intriguing opportunity [32–34]: in the strong exciton-photon coupling regime the system hosts hybrid quasiparticles, or polaritons, that share properties of both of their constituents [35]. Polariton modes are spectrally separated from the exciton-induced absorption peak, enabling large optical quality factors, while their excitonic component is extremely sensitive to strain fields owing to the large GaAs deformation potential [36–38], thus prospecting strong optomechanical interactions. Polaritons are bosonic quasiparticles which can form nonequilibrium condensates [39,40], while strong exciton-mediated nonlinearities enable the occurrence of superfluid behaviors [41,42], dissipative phase transitions [43,44], and parametric processes [45,46]. Optomechanical interactions offer an additional degree of freedom for quantum fluids of light foreshadowing new possibilities. Recent experiments showing mechanical lasing driven by a polariton condensate [47], the electrical actuation of polariton-phonon interactions [48], and giant polariton-induced bulk photoelastic effects [49,50], support this intuition, and call for the development of an unifying theoretical framework. Early works that established the foundations of polariton optomechanics, either focused on static effects and neglected the role of exciton-phonon and exciton-exciton interactions [51], or studied a two-level atom strongly coupled to an optomechanical cavity [52,53].

Here, we model the tripartite interaction of light, QW excitons, and sound in semiconductor microresonators. In the strong exciton-photon coupling regime, we show that such interaction generates a radiation-pressure type Hamiltonian, with photons replaced by polaritons, and with

an effective optomechanical coupling given by the weighted sum of the photon-phonon and exciton-phonon couplings. We provide analytical derivations of the effective optomechanical coupling for three resonator architectures: when considering parameters complying with current GaAs technologies, because of the giant exciton-phonon contribution, we show that a near-unity cooperativity can be obtained for a single polariton excitation. Finally, we investigate how polariton nonlinearities modify dynamical backaction via squeezing.

Model.—We consider the coupled dynamics of three bosonic fields describing the optical cavity mode, QW excitons, and a mechanical degree of freedom. We restrict ourselves to a single-mode scenario, leaving the generalization to the multimode case to forthcoming works. Notice that the exciton bosonization implies that we neglect electronic phase-space filling effects [35]. The large exciton effective mass in GaAs enables us to neglect its dispersion for all in-plane optical wave vectors [54]. The bare system Hamiltonian reads ($\hbar = 1$)

$$\hat{H}_0 = \omega_c \hat{a}^\dagger \hat{a} + \omega_x \hat{d}^\dagger \hat{d} + \frac{g_{xx}}{2} \hat{d}^\dagger \hat{d}^\dagger \hat{d}\, \hat{d} + \Omega_m \hat{b}^\dagger \hat{b}, \quad (1)$$

where ω_c, ω_x, and Ω_m denote the cavity (C), exciton (X), and mechanical (M) resonance frequencies associated with the bosonic ladder operators $\hat{a}$, $\hat{d}$, and $\hat{b}$, while the anharmonic term proportional to g_{xx} takes into account exciton exchange interactions [55]. The couplings among the three modes are captured by

$$\hat{H}_I = g_{cx}(\hat{a}^\dagger \hat{d} + \hat{d}^\dagger \hat{a}) - g_{cm} \hat{a}^\dagger \hat{a}(\hat{b} + \hat{b}^\dagger) - g_{xm} \hat{d}^\dagger \hat{d}(\hat{b} + \hat{b}^\dagger). \quad (2)$$

The first term describes dipole photon-exciton interactions ($\omega_c \approx \omega_x \gg g_{cx}$), while the other two describe the parametric modulation of the C and X resonances actuated by the mechanical field ($g_{cm,xm} \ll \omega_{c,x}$) [19]. The coupling g_{cm} contains both geometric-deformation and photoelastic effects [27], while g_{xm} accounts for the exciton-phonon interaction via the deformation potential [37], see Fig. 1(a). We denote the C, (nonradiative) X, and M decay rates κ_c, κ_x, and Γ. In the strong C-X coupling regime ($g_{cx} \gg \kappa_{c,x}$), the normal modes of the light-matter Hamiltonian in the single-excitation subspace form the relevant basis. The bare X and C modes hybridize yielding the lower (L) and upper (U) polariton resonances $2\omega_{l,u} = (\omega_c + \omega_x) \mp \sqrt{\delta_{cx}^2 + 4g_{cx}^2}$, with $\delta_{cx} = (\omega_c - \omega_x)$. Polaritons are described by ladder operators $(\hat{u}, \hat{l})^T = \mathcal{R}[\theta_{cx}](\hat{d}, \hat{a})^T$ where $\mathcal{R}[\theta_{cx}]$ is a rotation with mixing angle θ_{cx} satisfying $\cos 2\theta_{cx} = -\delta_{cx}/\sqrt{\delta_{cx}^2 + 4g_{cx}^2}$. As a result, phonons effectively couple to L via $g_{lm} = (g_{xm}\sin^2\theta_{cx} + g_{cm}\cos^2\theta_{cx})$, and to U via $g_{um} = (g_{xm}\cos^2\theta_{cx} + g_{cm}\sin^2\theta_{cx})$. In the polariton basis $\hat{H}_0 + \hat{H}_I = \hat{H}_l + \hat{H}_u + \hat{H}_m + \hat{H}_{lu}$, where

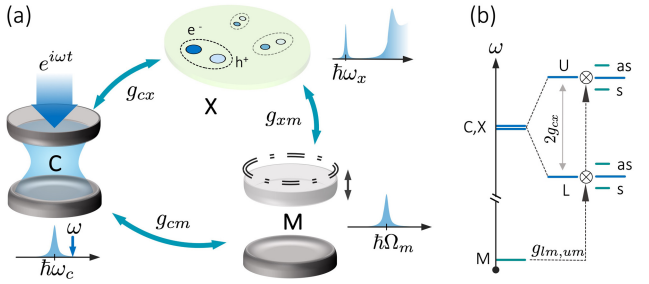

FIG. 1. (a) A resonator supports optical and mechanical modes with respective frequencies ω_c and Ω_m. It also embeds a quantum well (QW) with excitonic resonance at $\omega_x \approx \omega_c$. The cavity is driven by a laser with frequency ω. We denote g_{ij} the pairwise couplings among the modes. (b) Energy level diagram. Strong exciton-photon coupling results in a Rabi splitting $\Omega_R \approx 2g_{cx}$ between the upper (U) and lower (L) polariton normal modes. The mechanical mode modulates the polariton resonances through the effective couplings g_{lm} and g_{um}, producing Stokes (s) and anti-Stokes (as) sidebands.

$$\hat{H}_{j=(l,u)} = \left[\omega_j + \frac{\chi_j}{2}(\hat{n}_j - 1) - g_{jm}(\hat{b} + \hat{b}^\dagger)\right]\hat{n}_j \quad (3)$$

describes interacting polaritons in the L and U branches that are parametrically coupled to a mechanical mode. Here, $\hat{n}_j$ denote number operators, $\chi_l = g_{xx}\sin^4\theta_{cx}$, $\chi_u = g_{xx}\cos^4\theta_{cx}$, $\hat{H}_m = \Omega_m \hat{b}^\dagger \hat{b}$, and $\hat{H}_{lu} = -g_{lu}(\hat{b} + \hat{b}^\dagger)(\hat{l}^\dagger \hat{u} + \hat{u}^\dagger \hat{l})$ is a mechanically assisted coupling between the L and U polariton branches, with $g_{lu} = \sin(2\theta_{cx})(g_{xm} - g_{cm})/2$. We sketch the energy levels for the coupled CXM system in Fig. 1(b). Interestingly, $\hat{H}_{lu}$ describes a coherent three wave mixing among the polariton branches mediated by phonons, becoming resonant as the mechanical frequency matches the normal mode splitting $\Omega_m = \sqrt{\delta_{cx}^2 + 4g_{cx}^2}$, enabling a coherent population transfer [56]. Hereafter, we consider driving coherently C using a narrow-band laser of frequency ω, see Fig. 1(a).

Electromechanical coupling.—Exciton-phonon coupling stems from the strain-induced perturbation of the semiconductor band structure [37]. The resulting exciton energy shift is given by $U(\boldsymbol{r}_e, \mathbf{r}_h) = a_e \Sigma_n(\boldsymbol{r}_e) - a_h \Sigma_n(\boldsymbol{r}_h)$ [38], where $a_{e,h}$ are the electron and hole deformation potentials and $\Sigma_n(\boldsymbol{r}) = \nabla \cdot \boldsymbol{u}_n(\boldsymbol{r})$ denotes the volumetric strain at the position $\boldsymbol{r}$ imputable to a phonon in the mode n associated with the displacement field $\boldsymbol{u}_n(\boldsymbol{r})$. Upon tracing $U(\boldsymbol{r}_e, \boldsymbol{r}_h)$ in the exciton and phonon basis, as the exciton Bohr radius is much smaller than the phonon wavelength in the QW plane (cf. [57]), the electromechanical coupling reduces to

$$g_{xm}^{(n,m)} \approx (a_h - a_e) \int_S d\boldsymbol{R} |E_m(\boldsymbol{R})|^2 \Sigma_n(\boldsymbol{R}, z_{\mathrm{QW}}), \quad (4)$$

where $\boldsymbol{R}$ is the vector spanning the QW plane over the horizontal cross section S of the resonator, z_{QW} is the

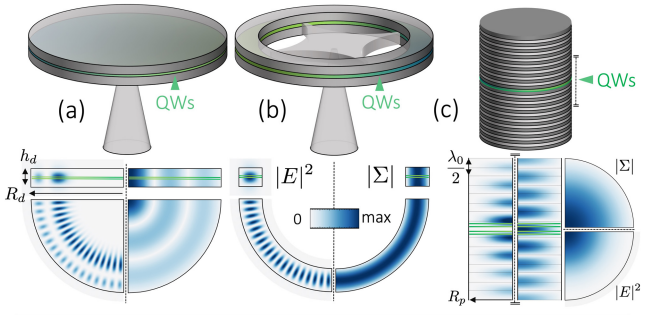

$\Omega_m/2\pi$	2.9	4.1	19.6	GHz
$g_{xm}/2\pi$	2.3	5.5	24.2	MHz
$g_{cm}/2\pi$	$0.6-1.1$	$1.1-2.3$	$0.1-0.3$	MHz
$g_{cx}/2\pi$	1.03	1.03	0.53	THz

FIG. 2. Sketch of a disk (a), ring (b), and pillar (c) microresonator. Here, (a), (b) are 0.2 μm thick with an outer radius $R_d = 2$ μm; in (b) the inner radius is 1.5 μm. (c) is 2.6 μm in diameter and defined by two GaAs/AlAs distributed Bragg reflectors (DBRs) and $\lambda/2$ GaAs spacer. All structures are adjusted to yield optical resonances near $E_x = 1.463$ eV (for a 8 nm thick $In_{0.05}Ga_{0.95}As$ QW [57]). Normalized intensity profiles of a cavity mode ($|E|^2$) and strain field ($|\Sigma|$) are shown for in-plane and orthogonal cuts. The QW positions are highlighted with solid lines: in (a), (b) two QWs are displaced by ± 15 nm from the cavity field antinode ($\eta_S \approx 1$), whereas in (c) 4 QWs displaced by $\pm(15, 39)$ nm from the center of the spacer $\eta_S = (0.93, 0.62)$. The calculated M frequency ($\Omega_m/2\pi$) and coupling rates ($g_{ij}/2\pi$) are listed for the selected modes. We list $g_{cm}/2\pi$ for a cavity mode detuning of 40–10 nm from the GaAs band gap. Information on the optical and mechanical decay rates can be found in [57].

position of the QW along the vertical axis, and $E_m(\boldsymbol{R})$ is the electric field distribution for the mth optical mode at the QW plane. In the strong coupling regime the optical mode enters the overlap integral as the exciton density is dictated by the cavity field profile [54]. We now evaluate Eq. (4) for the three microresonator geometries presented in Fig. 2: disk (a), ring (b), and pillar (c) microresonators. For each architecture, Fig. 2 shows representative profiles of the optical and strain fields presenting a near-optimal overlap. We could find analytical expressions for the mode envelopes and recast Eq. (4) as $\hbar g_{xm}^{(n,m)} = (a_e - a_h)(x_{\mathrm{ZPF}} k_m)\mathcal{I}_g \eta_S$ where x_{ZPF} is the zero-point fluctuation amplitude, k_m is the phonon wave vector, $\mathcal{I}_g$ is a geometric overlap integral, and η_S is the ratio between the peak value of the strain in the QW plane and its maximum (hence $\eta_S < 1$). As $|a_e - a_h| \approx 9.7$ eV for GaAs [38], we expect g_{xm} to be larger than g_{cm}, sharing a similar expression but a prefactor proportional to $\hbar\omega_c$ [27,85].

In [57], we compute $\mathcal{I}_g$ for any radial breathing mode (RBM) and any whispering gallery mode (WGM) for resonators (a), (b), while for the fundamental optical and longitudinal breathing mode of (c) we find

$$\mathcal{I}_g \approx \beta_0 \exp\left(\Delta n / 2 n_{\mathrm{eff}}\right)/\pi J_1(\alpha_{01}). \tag{5}$$

Here, $\beta_0 \approx 1.18$, $J_n(r)$ is the Bessel function of first kind, α_{01} is the first zero of J_0, $n_{\mathrm{eff}} = 3.2$ is the effective refractive index of the heterostructure; $\Delta n = 0.6$ and λ_0 are the index contrast and central wavelength of the DBRs, and $k_m = 2\pi n_{\mathrm{eff}}/\lambda_0$. Figure 2 lists g_{xm} for the modes indicated in the density maps. The values of g_{cm} were extracted adapting [27,85], while g_{cx} can be calculated as in [54,86] (cf. [57]). For the near-optimal $\mathcal{I}_g$ values here considered, we notice that the ratio $g_{xm}/\Omega_m \sim 10^{-3}$ is independent of the resonator geometry. Indeed, higher Ω_m values lead to shorter phonon wavelengths, and larger displacement gradients efficiently activate the deformation potential. As pillars here support the highest phonon frequencies, they present the largest optomechanical coupling ratio $g_{xm}/g_{cm} \sim 10^2$. Related findings for disk and ring resonators are discussed in [57], as a function of the C and M mode indices, showing overall that polaritons experience strongly enhanced optomechanical interactions.

As an example, we compute the single polariton cooperativity ($C_0 = 4g_{lm}^2/\kappa_l\Gamma$) for the resonator in Fig. 2(c) as a function of the pillar radius R_p. Deriving the scaling of x_{ZPF} with R_p, and adapting the value of g_{cm} provided in [85], yields $g_{lm}(R_p)$. The optical decay rate of the heterostructure, including residual absorption at 4 K [87], reaches $\kappa_c/2\pi \approx 7.2$ GHz for 25 DBR pairs (i.e., a quality factor $Q_c \sim 5 \times 10^4$). We also consider a nonradiative exciton decay rate $\kappa_x/2\pi = 4.8$ GHz [88], and recall that $\kappa_l = \cos^2\theta_{cx}\kappa_c + \sin^2\theta_{cx}\kappa_x$ [86]. Because of the co-localization of C and M modes one expects $Q_m \approx Q_c$; several mechanisms can degrade Q_m [31,57]: we take $\Gamma/2\pi = 0.65$ MHz ($Q_m \approx Q_c/2$). Given the moderate Q factors at play, we neglect fabrication-induced surface losses. Figure 3(a) shows the cooperativity as a function of the pillar radius and exciton fraction. Interestingly, we observe a region where $C_0 \sim 1$. Nevertheless, such a regime is accessible only for large X fractions where detrimental effects related to the matter component become sizable [89,90]. In particular, the X transition always presents some inhomogeneous broadening. Using the theory developed in [91] we show in Fig. 3(b) to which extent this affects C_0, while Fig. 3(c) present the polariton inhomogeneous-broadening Γ_{inh} normalized to the mechanical damping Γ. We have considered a Gaussian broadening with full width at half maximum (FWHM) of 0.5–1.5 meV and $R_p = 0.7$ μm. Coherent control of M requires negligible added phase noise in the L mode, thus desirably $\Gamma_{\mathrm{inh}}/\Gamma < 1$ [92]. Remarkably, Figs. 3(b) and 3(c) indicate that state-of-the-art QWs with a broadening below 0.5 meV [93], allow coherent control with $C_0 \sim 1$ ($C_q \sim 0.3$ at 4 K) for resonators complying with current fabrication technologies. Quantum cavity optomechanics experiments would thus become feasible using few photons [94–96] while piezoeffects [97] may be harnessed to operate such resonators as transducers [12–14].

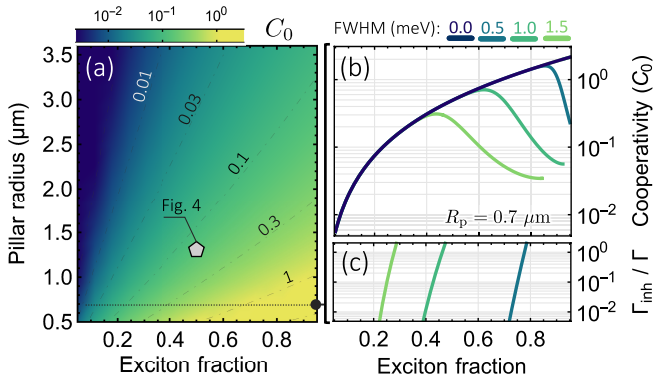

FIG. 3. (a) Single-polariton cooperativity versus exciton fraction and pillar radius (R_p). (b) Cut through panel (a) for $R_p = 0.7\ \mu$m showing the effect of inhomogeneous X broadening (Gaussian linewidth indicated in the inset). (c) Polariton inhomogeneous-broadening Γ_{inh}, relative to the mechanical damping Γ.

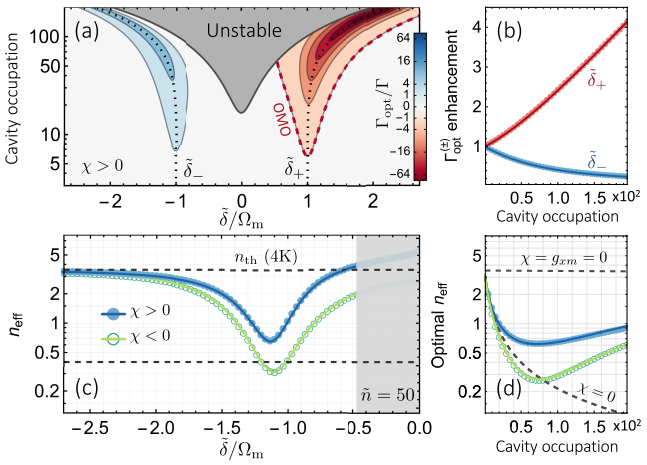

FIG. 4. (a) Optomechanical damping rate Γ_{opt} versus detuning ($\tilde{\delta}$), and photon occupation ($\tilde{n}$) for repulsive interactions ($\chi > 0$). Dashed black (red) lines trace the sideband detuning $\tilde{\delta}_\pm$ (the mechanical-oscillation threshold, OMO); unstable regions are shaded in gray. (b) Enhancement of $\Gamma^{\pm}_{opt}$ at the sidebands $\tilde{\delta}_\pm$ relative to its value for $\chi = 0$ as a function of the cavity occupation. (c) Mean phonon occupation n_{eff} versus detuning for $\tilde{n} = 50$. Dashed lines indicate the thermal population and the lowest n_{eff} for $\chi = 0$. (d) Minimal n_{eff} versus the cavity occupation. In (b)–(d) markers denote numerical solutions while lines show the analytical results [57].

Dynamics.—Finally, we study how polariton nonlinearities modify dynamical backaction. We consider $g_{cx}/\Omega_m \gg 1$, then $\hat{H}_{lu}$ is off resonant and the dynamics of the two polariton branches decouples. For a laser detuning $\delta = (\omega - \omega_l) \ll g_{cx}$, we effectively obtain the Hamiltonian of a Kerr resonator coupled to a mechanical mode. In [57], we derive the quantum Langevin equations (QLEs) ruling the dynamics, calculate the steady-state observables and the regions of dynamical stability in parameter space. Provided single-polariton nonlinearities are weak ($\chi_l/\kappa_l \ll 1$), one can follow the standard linearization approach to study the dynamics of small fluctuations [98–100]. Because of the nonlinear term in Eq. (3), the L fluctuations $(\delta\hat{\alpha}, \delta\hat{\alpha}^\dagger)$ are dynamically coupled. Following [101], we introduce squeezed displacement operators $\hat{s} = \cosh(r)(\tilde{\alpha}^*\delta\hat{\alpha}) + \sinh(r)(\tilde{\alpha}\delta\hat{\alpha}^\dagger)$ where $\tilde{\alpha} = \langle\hat{l}\rangle$, $2r = \operatorname{arctanh}(-\chi\tilde{n}/\tilde{\delta})$, $\tilde{n} = |\tilde{\alpha}|^2$, $\tilde{\delta} = (\omega - \omega_l - 2\tilde{\chi}\,\tilde{n})$, and $\tilde{\chi} = (\chi_l - 2g_{lm}^2/\Omega_m)$. The squeezing transformation reduces the QLEs to those of an equivalent harmonic resonator, with a rescaled detuning $\delta_s = \tilde{\delta}\cosh(2r) + \chi_l\tilde{n}\sinh(2r)$, optomechanical coupling $g_s = g_{lm}e^{-r}$ and subject to a squeezed optical bath [57]. Accordingly, the modified mechanical susceptibility adopts the usual expression [19] upon introducing (δ_s, g_s), while the displacement spectrum $\bar{S}_{qq}(\omega)$ includes corrections due to correlations in the optical bath [57].

As an example, in Fig. 4 we employ this formalism to describe optomechanical amplification and cooling for the pillar indicated by the marker in Fig. 3(a). According to our previous results, we have $\kappa_l/2\pi = 6.5$ GHz, $\Omega_m/\kappa_l = 3$, $\Gamma/\kappa_l = 10^{-4}$, $g_{lm}/\kappa_l = 0.002$, and $\chi_l/\kappa_l = 0.03$ (cf. [57]), yielding a cooperativity $C_0 = 0.15$. We consider the system to be precooled to 4 K. Figure 4(a) presents the optomechanical damping rate Γ_{opt} as a function of the effective laser detuning from the L resonance ($\tilde{\delta}$), and of the polariton occupation; regions of single-mode instability are shaded in gray. The optomechanical self-oscillation threshold (OMO) is indicated with a dashed red line. We can observe two main differences with respect to the harmonic resonator case ($\chi = 0$). First, the sideband positions $\tilde{\delta}_\pm$ depend on the polariton density as $\tilde{\delta}_\pm \approx \pm\sqrt{\Omega_m^2 + \tilde{\chi}^2\tilde{n}^2}$ (assuming $\Omega_m/\kappa_l \gg 1$). Second, the extremal values of the optomechanical damping, denoted $\Gamma^{\pm}_{opt}$ are asymmetric: for repulsive $\chi > 0$ (attractive $\chi < 0$) nonlinearities the Stokes sideband is suppressed (enhanced) with respect to its value in the absence of nonlinearities; the opposite holds for the anti-Stokes sideband. Repulsive interactions boost the optomechanical gain, resulting in efficient ultralow threshold OMOs (here as low as $\tilde{n} \approx 7$). Quantitatively, assuming $\Gamma_{opt}(\omega) \approx \Gamma_{opt}(\Omega_m)$, yields the sideband enhancement factor $\eta_\pm = (1 + \chi\tilde{n}/\tilde{\delta}_\pm)^{1/2}/(1 + \chi\tilde{n}/\tilde{\delta}_\mp)^{1/2}$, traced with solid lines in Fig. 4(b) versus cavity occupation for $\chi_l > 0$; markers indicate the results obtained by exact diagonalization of the QLEs [57].

Concerning the cooling performance, we start by noticing that the mean effective phonon occupation in the system (n_{eff}) is related to the internal energy of the oscillator $\Omega_m(n_{eff} + 1/2) = \int(d\omega/4\pi)\tilde{m}(\Omega^2 + \omega^2)\bar{S}_{qq}(\omega)$ [99]. In Fig. 4(c) we trace n_{eff} as a function of laser detuning for $\tilde{n} = 50$, both for the case of repulsive (solid markers) and equal but attractive (hollow markers) nonlinearities. In both cases occupations below unity can be achieved. As the Stokes sideband is reduced (enhanced) when $\chi > 0$ ($\chi < 0$) with respect to the linear case ($\chi = 0$), one would expect

cooling protocols to be more efficient for $\chi < 0$. In Fig. 4(e) we trace the minimum achievable n_{eff} versus cavity occupation for the three cases, showing this is not generally true. For large interaction energies $\tilde{\chi}\,\tilde{n} \sim \kappa$, even if the sideband enhancement factor η_- becomes large, the sideband peak detunes from Ω_m (unaffected by optical nonlinearities) thus suppressing the scattering rate by $\sim \kappa_l^2[4(\Omega_m - \tilde{\delta}_-)^2 + \kappa_l^2]^{-1}$. For the specific resonator considered in Fig. 4, these two opposing effects result in a finite yet modest improvement of the cooling performance. Nevertheless, our analytic results indicate that the cooling enhancement becomes large in the bad cavity limit, see [57,100,102]. Furthermore, to ease the comparison with the linear case, we kept g_{xm} constant. In practice, without excitons, $\chi_l = g_{xm} = 0$ and a $(g_{lm}/g_{cm})^2 \sim 10^3$ higher cavity occupation is required to reach $n_{\mathrm{eff}} \sim 1$, see Fig. 4(d). Finally, we notice that for large cavity occupations ($\tilde{n} \sim 10^3$), one enters the strong optomechanical coupling regime [57,103,104], characterized by hybrid *M-C-X* quasiparticles, or phonoritons, akin to those predicted for cavities embedding *h*-BN flakes [105], or two-level atoms [53].

Outlook.—Our results demonstrate the potential of harnessing QW exciton polaritons to enhance optomechanical interactions and indicate that a near-unity single-polariton cooperativity can be achieved in state-of-the-art resonators. Contextually, we adapted the theory of dynamical backaction to include polariton interactions and showed that sideband cooling at 4 K is sufficient for ground-state preparation. We foresee that stronger nonlinearities [89,90] could be exploited to stabilize nonclassical mechanical states [11]. Our analysis can be readily extended to multimode scenarios, naturally emerging in coupled microresonator arrays, where a simultaneous engineering of the polariton and phonon dispersion would disclose a variety of applications [106–108].

This work was supported by the MaCaCQu Flagship project of the Paris Saclay Labex (ANR-10-LABX-0035), by ANR via the project UNIQ, by the H2020-FETFLAG project PhoQus (820392), by the QUANTERA project Interpol (ANRQUAN-0003-05), and by the European Research Council via the project ARQADIA (949730), and the Consolidator grant NOMLI (770933). We thank Daniel Lanzillotti-Kimura and Philippe St-Jean for valuable discussions as well as Jérémy Bon for numerical assistance.

[*]These authors contributed equally to this work.
[†]Corresponding author.
carlonn@ethz.ch
[‡]Corresponding author.
zakari.denis@univ-paris-diderot.fr
[‖]Present address: Photonics Laboratory, ETH Zürich, 8093 Zürich, Switzerland.

[1] D. Mason, J. Chen, M. Rossi, Y. Tsaturyan, and A. Schliesser, Nat. Phys. **15**, 745 (2019).
[2] N. Rossi, F. R. Braakman, D. Cadeddu, D. Vasyukov, G. Tütüncüoglu, A. Fontcuberta i Morral, and M. Poggio, Nat. Technol. **12**, 150 (2017).
[3] D. Hälg, T. Gisler, Y. Tsaturyan, L. Catalini, U. Grob, M.-D. Krass, M. Héritier, H. Mattiat, A.-K. Thamm, R. Schirhagl, E. C. Langman, A. Schliesser, C. L. Degen, and A. Eichler, Phys. Rev. Applied **15**, L021001 (2021).
[4] C. Dong, V. Fiore, M. C. Kuzyk, and H. Wang, Science **338**, 1609 (2012).
[5] T. P. Purdy, P.-L. Yu, R. W. Peterson, N. S. Kampel, and C. A. Regal, Phys. Rev. X **3**, 031012 (2013).
[6] W. Chen, P. Roelli, H. Hu, S. Verlekar, S. P. Amirtharaj, A. I. Barreda, T. J. Kippenberg, M. Kovylina, E. Verhagen, A. Martínez, and C. Galland, Science **374**, 1264 (2021).
[7] Y. Hu, S. Ding, Y. Qin, J. Gu, W. Wan, M. Xiao, and X. Jiang, Phys. Rev. Lett. **127**, 134301 (2021).
[8] T. P. Purdy, R. W. Peterson, and C. A. Regal, Science **339**, 801 (2013).
[9] I. Marinković, A. Wallucks, R. Riedinger, S. Hong, M. Aspelmeyer, and S. Gröblacher, Phys. Rev. Lett. **121**, 220404 (2018).
[10] U. Delić, M. Reisenbauer, K. Dare, D. Grass, V. Vuletić, N. Kiesel, and M. Aspelmeyer, Science **367**, 892 (2020).
[11] X. Ma, J. J. Viennot, S. Kotler, J. D. Teufel, and K. W. Lehnert, Nat. Phys. **17**, 322 (2021).
[12] A. P. Higginbotham, P. S. Burns, M. D. Urmey, R. W. Peterson, N. S. Kampel, B. M. Brubaker, G. Smith, K. W. Lehnert, and C. A. Regal, Nat. Phys. **14**, 1038 (2018).
[13] M. Mirhosseini, A. Sipahigil, M. Kalaee, and O. Painter, Nature (London) **588**, 599 (2020).
[14] G. Arnold, M. Wulf, S. Barzanjeh, E. S. Redchenko, A. Rueda, W. J. Hease, F. Hassani, and J. M. Fink, Nat. Commun. **11**, 4460 (2020).
[15] H. J. Kimble, Nature (London) **453**, 1023 (2008).
[16] R. Barends *et al.*, Nature (London) **508**, 500 (2014).
[17] N. Ofek, A. Petrenko, R. Heeres, P. Reinhold, Z. Leghtas, B. Vlastakis, Y. Liu, L. Frunzio, S. M. Girvin, L. Jiang, M. Mirrahimi, M. H. Devoret, and R. J. Schoelkopf, Nature (London) **536**, 441 (2016).
[18] A. A. Clerk, K. W. Lehnert, P. Bertet, J. R. Petta, and Y. Nakamura, Nat. Phys. **16**, 257 (2020).
[19] M. Aspelmeyer, T. J. Kippenberg, and F. Marquardt, Rev. Mod. Phys. **86**, 1391 (2014).
[20] L. Ding, C. Baker, P. Senellart, A. Lemaitre, S. Ducci, G. Leo, and I. Favero, Appl. Phys. Lett. **98**, 113108 (2011).
[21] S. Anguiano, A. E. Bruchhausen, B. Jusserand, I. Favero, F. R. Lamberti, L. Lanco, I. Sagnes, A. Lemaître, N. D. Lanzillotti-Kimura, P. Senellart, and A. Fainstein, Phys. Rev. Lett. **118**, 263901 (2017).
[22] H. Ren, M. H. Matheny, G. S. MacCabe, J. Luo, H. Pfeifer, M. Mirhosseini, and O. Painter, Nat. Commun. **11**, 3373 (2020).
[23] A. D. O'Connell, M. Hofheinz, M. Ansmann, R. C. Bialczak, M. Lenander, E. Lucero, M. Neeley, D. Sank, H. Wang, M. Weides, J. Wenner, J. M. Martinis, and A. N. Cleland, Nature (London) **464**, 697 (2010).

[24] A. H. Safavi-Naeini, J. Chan, J. T. Hill, T. P. Mayer Alegre, A. Krause, and O. Painter, Phys. Rev. Lett. **108**, 033602 (2012).

[25] M. Rossi, D. Mason, J. Chen, Y. Tsaturyan, and A. Schliesser, Nature (London) **563**, 53 (2018).

[26] Y.-D. Wang and A. A. Clerk, Phys. Rev. Lett. **108**, 153603 (2012).

[27] C. Baker, W. Hease, D.-T. Nguyen, A. Andronico, S. Ducci, G. Leo, and I. Favero, Opt. Express **22**, 14072 (2014).

[28] A. Feldman and D. Horowitz, J. Appl. Phys. **39**, 5597 (1968).

[29] A. Barg, L. Midolo, G. Kiršanskė, P. Tighineanu, T. Pregnolato, A. İmamoğlu, P. Lodahl, A. Schliesser, S. Stobbe, and E. S. Polzik, Phys. Rev. B **98**, 155316 (2018).

[30] R. Lifshitz and M. L. Roukes, Phys. Rev. B **61**, 5600 (2000).

[31] M. Hamoumi, P. E. Allain, W. Hease, E. Gil-Santos, L. Morgenroth, B. Gérard, A. Lemaître, G. Leo, and I. Favero, Phys. Rev. Lett. **120**, 223601 (2018).

[32] A. Fainstein, N. D. Lanzillotti-Kimura, B. Jusserand, and B. Perrin, Phys. Rev. Lett. **110**, 037403 (2013).

[33] G. Rozas, A. E. Bruchhausen, A. Fainstein, B. Jusserand, and A. Lemaître, Phys. Rev. B **90**, 201302(R) (2014).

[34] V. Villafañe, P. Sesin, P. Soubelet, S. Anguiano, A. E. Bruchhausen, G. Rozas, C. G. Carbonell, A. Lemaître, and A. Fainstein, Phys. Rev. B **97**, 195306 (2018).

[35] I. Carusotto and C. Ciuti, Rev. Mod. Phys. **85**, 299 (2013).

[36] J. Bardeen and W. Shockley, Phys. Rev. **80**, 72 (1950).

[37] G. L. Bir and G. E. Pikus, *Symmetry and Strain-Induced Effects in Semiconductors* (Wiley, New York, 1974).

[38] C. Piermarocchi, F. Tassone, V. Savona, A. Quattropani, and P. Schwendimann, Phys. Rev. B **53**, 15834 (1996).

[39] J. Kasprzak, M. Richard, S. Kundermann, A. Baas, P. Jeambrun, J. M. J. Keeling, F. M. Marchetti, M. H. Szymańska, R. André, J. L. Staehli, V. Savona, P. B. Littlewood, B. Deveaud, and L. S. Dang, Nature (London) **443**, 409 (2006).

[40] H. Deng, H. Haug, and Y. Yamamoto, Rev. Mod. Phys. **82**, 1489 (2010).

[41] A. Amo, J. Lefrère, S. Pigeon, C. Adrados, C. Ciuti, I. Carusotto, R. Houdré, E. Giacobino, and A. Bramati, Nat. Phys. **5**, 805 (2009).

[42] G. Lerario, A. Fieramosca, F. Barachati, D. Ballarini, K. S. Daskalakis, L. Dominici, M. De Giorgi, S. A. Maier, G. Gigli, S. Kéna-Cohen, and D. Sanvitto, Nat. Phys. **13**, 837 (2017).

[43] S. R. K. Rodriguez, W. Casteels, F. Storme, N. Carlon Zambon, I. Sagnes, L. Le Gratiet, E. Galopin, A. Lemaître, A. Amo, C. Ciuti, and J. Bloch, Phys. Rev. Lett. **118**, 247402 (2017).

[44] T. Fink, A. Schade, S. Höfling, C. Schneider, and A. Imamoglu, Nat. Phys. **14**, 365 (2018).

[45] A. S. Kuznetsov, G. Dagvadorj, K. Biermann, M. H. Szymanska, and P. V. Santos, Optica **7**, 1673 (2020).

[46] N. Carlon Zambon, S. R. K. Rodriguez, A. Lemaître, A. Harouri, L. Le Gratiet, I. Sagnes, P. St-Jean, S. Ravets, A. Amo, and J. Bloch, Phys. Rev. A **102**, 023526 (2020).

[47] D. L. Chafatinos, A. S. Kuznetsov, S. Anguiano, A. E. Bruchhausen, A. A. Reynoso, K. Biermann, P. V. Santos, and A. Fainstein, Nat. Commun. **11**, 4552 (2020).

[48] A. S. Kuznetsov, D. H. O. Machado, K. Biermann, and P. V. Santos, Phys. Rev. X **11**, 021020 (2021).

[49] B. Jusserand, A. N. Poddubny, A. V. Poshakinskiy, A. Fainstein, and A. Lemaitre, Phys. Rev. Lett. **115**, 267402 (2015).

[50] M. Kobecki, A. V. Scherbakov, S. M. Kukhtaruk, D. D. Yaremkevich, T. Henksmeier, A. Trapp, D. Reuter, V. E. Gusev, A. V. Akimov, and M. Bayer, Phys. Rev. Lett. **128**, 157401 (2022).

[51] O. Kyriienko, T. C. H. Liew, and I. A. Shelykh, Phys. Rev. Lett. **112**, 076402 (2014).

[52] J. Restrepo, C. Ciuti, and I. Favero, Phys. Rev. Lett. **112**, 013601 (2014).

[53] J. Restrepo, I. Favero, and C. Ciuti, Phys. Rev. A **95**, 023832 (2017).

[54] G. Panzarini and L. C. Andreani, Phys. Rev. B **60**, 16799 (1999).

[55] C. Ciuti, V. Savona, C. Piermarocchi, A. Quattropani, and P. Schwendimann, Phys. Rev. B **58**, 7926 (1998).

[56] E. S. Vyatkin and A. N. Poddubny, Phys. Rev. B **104**, 075447 (2021).

[57] See Supplemental Material at http://link.aps.org/supplemental/10.1103/PhysRevLett.129.093603, including Refs. [58–84], for details on the analytical derivation of the exciton-phonon coupling in the three microresonator architechtures, on practical limitations to the optical and mechanical quality factors, on shallow quantum well excitons and on the theory of polariton dynamical backaction.

[58] A. I. Ansel'm and Iu. A. Firsov, Sov. Phys. JETP **1**, 139 (1955).

[59] C. Herring and E. Vogt, Phys. Rev. **101**, 944 (1956).

[60] A. Altland and B. D. Simons, *Condensed Matter Field Theory*, 2nd ed. (Cambridge University Press, Cambridge, 2010).

[61] S. Paul, J. B. Roy, and P. K. Basu, J. Appl. Phys. **69**, 827 (1991).

[62] V. I. Zubkov, M. A. Melnik, A. V. Solomonov, E. O. Tsvelev, F. Bugge, M. Weyers, and G. Tränkle, Phys. Rev. B **70**, 075312 (2004).

[63] G. Bastard, *Wave Mechanics Applied to Semiconductor Heterostructures*, Monographies de Physique (EDP Science, Les Ulis, France, 1992).

[64] M. Levinshtein, S. Rumyantsev, and M. Shur, *Si, Ge, C (Diamond), GaAs, GaP, GaSb, InAs, InP, InSb*, Handbook Series on Semiconductor Parameters Vol. 1 (World Scientific, Singapore, 1996).

[65] S. Adachi, J. Appl. Phys. **53**, 8775 (1982).

[66] K. J. Moore, G. Duggan, K. Woodbridge, and C. Roberts, Phys. Rev. B **41**, 1090 (1990).

[67] L. C. Andreani, in *Confined Electrons and Photons* edited by E. Burstein and C. Weisbuch (Springer, Boston, 1995), Vol. 340, pp. 57–112.

[68] J. W. Strutt, *The Theory of Sound*, Cambridge Library Collection–Physical Sciences Vol. 2 (Cambridge University Press, Cambridge, 2011).

[69] L. Rayleigh, London, Edinburgh, Dublin Philos. Mag. J. Sci. **20**, 1001 (1910).

[70] L. Rayleigh, London, Edinburgh, Dublin Philos. Mag. J. Sci. **27**, 100 (1914).

[71] L. D. Landau, E. M. Lifšic, and L. D. Landau, *Theory of Elasticity*, 3rd ed., Course of Theoretical Physics Vol. 7 (Elsevier, Amsterdam, 2008).

[72] D. Parrain, Optomécanique fibrée des disques GaAs: Dissipation, amplification et non-linéarités, Ph.D. thesis, Paris 7, 2014.

[73] Z. Hao and F. Ayazi, Sens. Actuators A **134**, 582 (2007).

[74] G. Anetsberger, R. Rivière, A. Schliesser, O. Arcizet, and T. J. Kippenberg, Nat. Photonics **2**, 627 (2008).

[75] R. Girlanda, A. Quattropani, and P. Schwendimann, Phys. Rev. B **24**, 2009 (1981).

[76] C. E. Whittaker, E. Cancellieri, P. M. Walker, D. R. Gulevich, H. Schomerus, D. Vaitiekus, B. Royall, D. M. Whittaker, E. Clarke, I. V. Iorsh, I. A. Shelykh, M. S. Skolnick, and D. N. Krizhanovskii, Phys. Rev. Lett. **120**, 097401 (2018).

[77] C. Yeh, L. Casperson, and W. P. Brown, Appl. Phys. Lett. **34**, 460 (1979).

[78] M. A. M. Marte and S. Stenholm, Phys. Rev. A **56**, 2940 (1997).

[79] B. D. Hauer, C. Doolin, K. S. D. Beach, and J. P. Davis, Ann. Phys. (Amsterdam) **339**, 181 (2013).

[80] M. Karl, B. Kettner, S. Burger, F. Schmidt, H. Kalt, and M. Hetterich, Opt. Express **17**, 1144 (2009).

[81] T. J. Kippenberg, H. Rokhsari, T. Carmon, A. Scherer, and K. J. Vahala, Phys. Rev. Lett. **95**, 033901 (2005).

[82] P. D. Drummond and D. F. Walls, J. Phys. A **13**, 725 (1980).

[83] J. B. Clark, F. Lecocq, R. W. Simmonds, J. Aumentado, and J. D. Teufel, Nature (London) **541**, 191 (2017).

[84] F. Marquardt, J. P. Chen, A. A. Clerk, and S. M. Girvin, Phys. Rev. Lett. **99**, 093902 (2007).

[85] S. Anguiano, P. Sesin, A. E. Bruchhausen, F. R. Lamberti, I. Favero, M. Esmann, I. Sagnes, A. Lemaître, N. D. Lanzillotti-Kimura, P. Senellart, and A. Fainstein, Phys. Rev. A **98**, 063810 (2018).

[86] V. Savona, *Confined Photon Systems: Fundamentals and Applications Lectures from the Summerschool Held in Cargèse, Corsica, 3–15 August 1998*, edited by H. Benisty, C. Weisbuch, É. Polytechnique, J.-M. Gérard, R. Houdré, J. Rarity, R. Beig, J. Ehlers, U. Frisch, K. Hepp, R. L. Jaffe, R. Kippenhahn, I. Ojima, H. A. Weidenmüller, J. Wess, J. Zittartz, and W. Beiglböck, Lecture Notes in Physics Vol. 531 (Springer Berlin Heidelberg, Berlin, Heidelberg, 1999).

[87] M. D. Sturge, Phys. Rev. **127**, 768 (1962).

[88] N. Carlon Zambon, Chirality and nonlinear dynamics in polariton microresonators, Ph.D. thesis, Université Paris-Saclay, 2020, https://tel.archives-ouvertes.fr/tel-03035028.

[89] A. Delteil, T. Fink, A. Schade, S. Höfling, C. Schneider, and A. İmamoğlu, Nat. Mater. **18**, 219 (2019).

[90] G. Muñoz-Matutano, A. Wood, M. Johnsson, X. Vidal, B. Q. Baragiola, A. Reinhard, A. Lemaître, J. Bloch, A. Amo, G. Nogues, B. Besga, M. Richard, and T. Volz, Nat. Mater. **18**, 213 (2019).

[91] I. Diniz, S. Portolan, R. Ferreira, J. M. Gérard, P. Bertet, and A. Auffèves, Phys. Rev. A **84**, 063810 (2011).

[92] P. Rabl, C. Genes, K. Hammerer, and M. Aspelmeyer, Phys. Rev. A **80**, 063819 (2009).

[93] S. V. Poltavtsev, Y. P. Efimov, Y. K. Dolgikh, S. A. Eliseev, V. V. Petrov, and V. V. Ovsyankin, Solid State Commun. **199**, 47 (2014).

[94] C. Galland, N. Sangouard, N. Piro, N. Gisin, and T. J. Kippenberg, Phys. Rev. Lett. **112**, 143602 (2014).

[95] N. Fiaschi, B. Hensen, A. Wallucks, R. Benevides, J. Li, T. P. M. Alegre, and S. Gröblacher, Nat. Photonics **15**, 817 (2021).

[96] F. Fogliano, B. Besga, A. Reigue, P. Heringlake, L. Mercier de Lépinay, C. Vaneph, J. Reichel, B. Pigeau, and O. Arcizet, Phys. Rev. X **11**, 021009 (2021).

[97] K. Fricke, J. Appl. Phys. **70**, 914 (1991).

[98] R. Bonifacio and L. A. Lugiato, Phys. Rev. Lett. **40**, 1023 (1978).

[99] C. Genes, D. Vitali, P. Tombesi, S. Gigan, and M. Aspelmeyer, Phys. Rev. A **77**, 033804 (2008).

[100] C. Laflamme and A. A. Clerk, Phys. Rev. A **83**, 033803 (2011).

[101] M. Asjad, N. E. Abari, S. Zippilli, and D. Vitali, Opt. Express **27**, 32427 (2019).

[102] D. Zoepfl, M. L. Juan, N. Diaz-Naufal, C. M. F. Schneider, L. F. Deeg, A. Sharafiev, A. Metelmann, and G. Kirchmair, arXiv:2202.13228.

[103] I. Yeo, P.-L. de Assis, A. Gloppe, E. Dupont-Ferrier, P. Verlot, N. S. Malik, E. Dupuy, J. Claudon, J.-M. Gérard, A. Auffèves, G. Nogues, S. Seidelin, J.-P. Poizat, O. Arcizet, and M. Richard, Nat. Technol. **9**, 106 (2014).

[104] M. Montinaro, G. Wüst, M. Munsch, Y. Fontana, E. Russo-Averchi, M. Heiss, A. Fontcuberta i Morral, R. J. Warburton, and M. Poggio, Nano Lett. **14**, 4454 (2014).

[105] S. Latini, U. De Giovannini, E. J. Sie, N. Gedik, H. Hübener, and A. Rubio, Phys. Rev. Lett. **126**, 227401 (2021).

[106] V. Peano, C. Brendel, M. Schmidt, and F. Marquardt, Phys. Rev. X **5**, 031011 (2015).

[107] W. H. P. Nielsen, Y. Tsaturyan, C. B. Møller, E. S. Polzik, and A. Schliesser, Proc. Natl. Acad. Sci. U.S.A. **114**, 62 (2017).

[108] F. Ruesink, J. P. Mathew, M.-A. Miri, A. Alù, and E. Verhagen, Nat. Commun. **9**, 1798 (2018).